ACS Photonics

Article

pubs.acs.org/journal/apchd5

Understanding the Interplay between Molecule Orientation and Graphene Using Polarized Raman Spectroscopy

Chiung-Yi Chen,[†,‡,§] Deniz P. Wong,[∥] Yi-Fan Huang,[†] Hsiang-Ting Lien,[†] Pei-Chun Chiang,[†] Pei-Ling Li,[∥] Fu-Yu Shih,[‡,∥] Wei-Hua Wang,[∥] Kuei-Hsien Chen,[†,∥] Li-Chyong Chen,*[,†] and Yang-Fang Chen*[,†,‡]

[†]Center for Condensed Matter Sciences and [‡]Department of Physics, National Taiwan University, Taipei 10617, Taiwan

[§]Nano Science and Technology Program, Taiwan International Graduate Program, Academia Sinica and National Taiwan University, Taipei, Taiwan

[∥]Institute of Atomic and Molecular Sciences, Academia Sinica, Taipei 106, Taiwan

Supporting Information

ABSTRACT: We present a systematic study in investigating the orientation characteristics of pentacene molecules grown on graphene substrates using polarized Raman spectroscopy. The substrate-induced orientation alignment of pentacene can be well distinguished through the polarized Raman spectra. Interestingly, we found that the nature of polycrystalline graphene not only provides efficient route to control molecular orientation, but also acts as an excellent template allowing conjugated molecules to stack accordingly. The relative orientation of the well-aligned pentacene molecules and the nearby graphene domains exhibits several preferred angles due to atomic interactions. This unique feature is further examined and verified by single domain graphene. Furthermore, polarized Raman spectroscopy contains abundant information allowing us to analyze the ordering level of pentacene films with various thicknesses, which provides insightful perspectives of manipulating molecular orientations with graphene and spatial organization between conjugated systems, in a more quantitative manner.

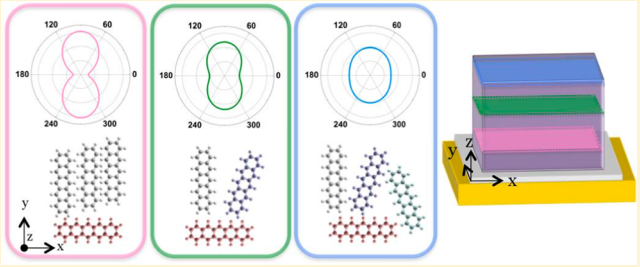

KEYWORDS: *polarized Raman spectroscopy, graphene domain, molecular orientation, pentacene*

Understanding and controlling molecular orientation has a significant impact on various physical properties of the molecules including their absorption coefficient, charge transport properties, and their corresponding performance in optoelectronic devices.[1,2] Numerous approaches have been conducted to have better control of the system.[3−5] It is therefore important to develop a practical method to gain insights regarding the underlying mechanisms for orientation control and providing a metrics for comparison. Several techniques have been used for characterizing molecular orientation such as X-ray diffraction (XRD) crystallography, Raman spectroscopy, and scanning tunneling microscope (STM).[6] Raman spectroscopy stands out as the most popular characterization tool for organic materials mainly because it is easily accessible, nondestructive, time-efficient, and non-vacuum-operated. Not only do we derive a collective behavior of atomic and electronic structure from Raman spectra,[7−9] but crystallographic orientation or grain boundaries could also be obtained[10−12] using polarization analysis.[13−15] Raman analysis uses specific vibration frequency of a molecule when light interacts with the corresponding phonon causing inelastic scattering. If the vibration mode is directional, it is possible to define its orientation in conjunction with polarized light, better known as polarized Raman spectroscopy. As a result, polarized Raman spectroscopic studies can provide detailed information on the distribution of crystal orientation with noninvasive and fast data acquisition.[16]

In this work, we report on the applications of polarized Raman spectroscopy in probing the orientation of pentacene molecules and their interaction with underlying graphene domains. Due to the interfacial $\pi-\pi$ interaction with conjugated molecules, previous studies[17,18] have shown that graphene and HOPG can be used as template to control molecular orientation. First, we study the effect of a polarized incident light on the Raman features of pentacene and how the changes in its molecular orientation change with its corresponding Raman spectra. Then, we study the distribution of pentacene molecules based on their preferred orientations on graphene layer produced from chemical vapor deposition (CVD) method. Interestingly, we found the orientation distribution correlates highly to the crystal domains of CVD graphene. In order to confirm our important findings, we have successfully examined the dependence between the molecular orientation of pentacene and the graphene domain using single crystal graphene obtained by mechanical exfoliation. Moreover,

Received: January 30, 2016
Published: May 16, 2016

DOI: 10.1021/acsphotonics.6b00074
ACS Photonics 2016, 3, 985−991

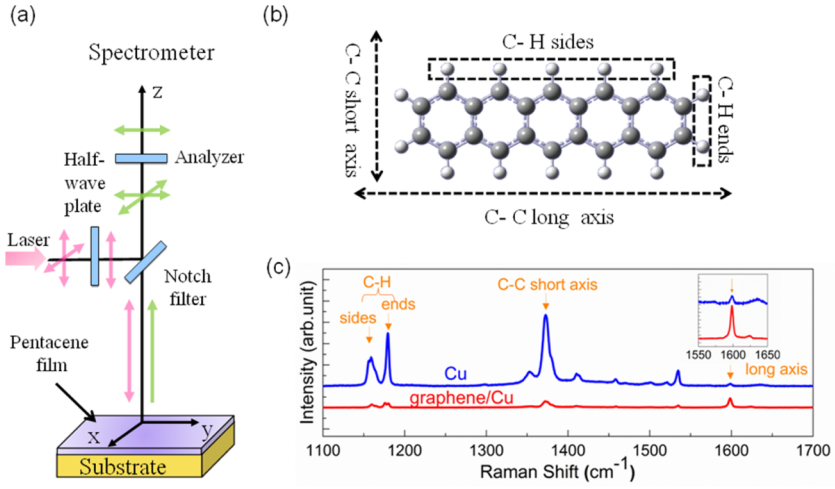

Figure 1. Schematic diagram of (a) the experimental setup following a backscattering geometry. The red and green arrows indicate the incident and scattered light polarizations, respectively. (b) Chemical structure of pentacene molecule. The dashed arrows and boxes illustrate the atoms involved and the vibrational directions of the molecule. (c) Typical Raman spectra of pentacene film of 50 nm on bare Cu and graphene/Cu. The main peaks are assigned by the indicated label. The inset in (c) reveals the magnification near the C−C long axis peak.

key parameters in resolving the level of anisotropy and isotropy in relation to the evolution of pentacene orientation with thickness are also elucidated. Thus, the present study not only demonstrates polarized Raman spectroscopy to be a facile method for characterizing pentacene and graphene domains, but also unravels the unique feature of molecular self-assembly due to its interaction with graphene. The approach presented here can be further applied to similar symmetrical systems.

RESULTS AND DISCUSSION

Polarized Raman Spectroscopy of Pentacene. The experimental geometry of polarized micro-Raman measurement is shown in Figure 1a. Pentacene[19,20] is a Raman active molecule with specific vibration modes (Figure 1b). There are four main vibration peaks in the range of 1100−1700 cm^{-1}, which can be attributed to C−H in-plane bending and the C−C aromatic stretching modes, as shown in the spectra (Figure 1c). The 1158 and 1178 cm^{-1} are associated with the displacement of H atoms located at the ends and sides of the pentacene molecule marked in dotted black boxes. For the C−C stretching modes, the peaks can be assigned as C−C short axis (1374 cm^{-1}) and C−C long axis (1598 cm^{-1}) modes. All of the main vibrational modes are consistent with previous reports.[21,22] It is worth noting that the relative peak intensity of C−C vibration mode is associated with molecular orientation with respect to the substrate, which has been used to probe the in-plane orientation of 6,13-bis(triisopropylsilylethynyl) pentacene (TIPS-pentacene) due to pentacene backbones lying on the substrate.[23] A closer examination of 1598 cm^{-1} for long axis vibration mode of pentacene molecules on graphene/Cu and bare Cu substrates is shown in Figure 1c. We can clearly see that, due to different molecular geometries on different substrates, the Raman intensity also changes. Because of stronger $\pi-\pi$ interaction[24,25] between pentacene and graphene, the molecules stack in a lying-down configuration[26−30] and the fused rings face the substrate.[3,31] Therefore, the peak intensity of C−C long axis is stronger on graphene/Cu substrate. On the other hand, the weak peak intensity of C−C long axis of pentacene on bare Cu substrate indicates that the molecules arrange in a standing-up configuration. Other reports have shown that graphene can act as a template for surface-enhanced Raman scattering of various molecules, however, as mentioned by Huang et al., pentacene is a molecule with small Raman cross sections with negligible Raman scattering efficiency on graphene.[32] Thus, the changes we observed in our Raman intensity comes from the intrinsic scattering of the pentacene molecule without any substrate enhancement.

Theoretical Background. To have a better understanding of the above result, let us examine the relation between polarization and Raman modes. The peak intensity of a Raman mode (I) is dominated by the crystal orientation (Raman tensor) and polarization geometry, which can be expressed as[33]

$$I \propto |\mathbf{e}_i \cdot \mathcal{R} \cdot \mathbf{e}_s|^2 \quad (1)$$

where $\mathbf{e}_i$ and $\mathbf{e}_s$ are the unit polarization vectors of the incident and scattered light, respectively and $\mathcal{R}$ defines the Raman tensor of a specific vibration mode. The variation of Raman intensity with respect to the in-plane rotation angle θ can be deduced by using eq 1, where both short axis (A_g) and long axis (B_{3g}) modes[34,35] follow $\cos^2(\theta)$ and $\sin^2(\theta)$, respectively (see Supporting Information, S1). The relations suggest the A_g mode reaches its maximum, while B_{3g} mode is in its minimum at 0°, and the two modes are in 90° out of phase. The C−C stretching modes of pentacene, therefore, provide a direct evidence for the molecular orientation and hence, will be the vibration mode of interest of our analysis.

Based on the discussion above, we can visualize molecular configurations and polarization dependence shown in Figure 2. As the light beam propagates vertically to the substrate, the electric field is polarized in $x-y$ plane at a certain direction. As shown in Figure 2a, pentacene molecules stand up with their backbones on the substrate and cover randomly over the surface. Under this condition, it is expected that both Raman intensities of C−C short axis and C−C long axis are insensitive to the in-plane polarization. Notice that the C−C long axis mode is inactive because of the standing-up orientation. On the other hand, if pentacene molecules lie down on the substrate (Figure 2b) and align well in a particular direction, it will induce the polarization dependence of C−C short axis and C−C long axis with 90° out of phase as expected from the geometry. Moreover, the intensities of C−C short and C−C long axes will vary as $\cos^2(\theta)$ and $\sin^2(\theta)$, respectively. This

DOI: 10.1021/acsphotonics.6b00074
ACS Photonics 2016, 3, 985−991

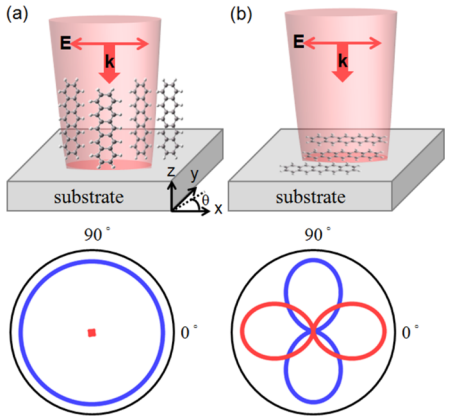

Figure 2. Schematic sketch of different molecular orientations of (a) standing-up and (b) lying-down pentacene molecules and their dependence with the polarization of incident beam, where **k** and **E** vectors indicate the propagation and polarization of electric field directions. Bottom panels illustrate the corresponding polar patterns, where the angle is defined in the $x-y$ plane and blue and red curves represent C−C short and C−C long axes, respectively.

result demonstrates that we are able to take advantage of the angle-dependent spectra to resolve the molecular configuration of pentacene molecules.

Polarized Raman Spectra of Pentacene on Graphene/Cu and Bare Cu Substrates. To confirm the above prediction, we have performed the polarization dependence of Raman spectra. Figure 3a is a series of Raman spectra of

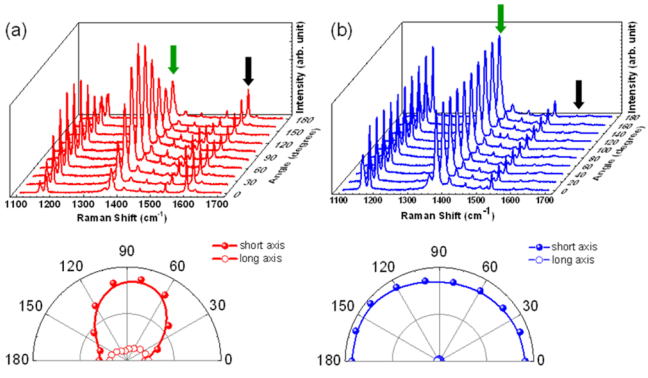

Figure 3. Polarized Raman spectra of pentacene films on (a) graphene/Cu and (b) bare Cu substrates. Each plot corresponds to different polarization states of the incident electric field rotated from 0 to 180° in steps of 20°. The polar patterns in lower panels depict the peak intensity of C−C short and C−C long axes in relation to each polarization state (indicated in green and black arrows, respectively) from the upper panels accordingly.

pentacene film (with a thickness of 50 nm) deposited on graphene/Cu substrate. Each spectrum was measured under different polarization angle as labeled in the figure. The main peaks clearly show high polarization anisotropy. Note that both C−C short axis and C−C long axis modes (indicated in green arrows) vary in a periodic way; as expected, they are 90° out of phase (it is shown to be nearly 90° out of phase, see Supporting Information, S2). To further understand the actual behavior of the C−C stretching modes, we extract intensities of the vibrational modes from the spectra and plot into a polar pattern. The fitted lines of short axis and long-axis are basically in accordance with $\sin^2(\theta)$ and $\cos^2(\theta)$, respectively. Our results suggest that there is a preferred orientation of pentacene molecules on graphene/Cu substrate. In order to verify whether the bare Cu substrate or the honeycomb structure of graphene plays the role as a template for pentacene molecules, we have also deposited pentacene film on bare Cu substrate under the same condition as shown in Figure 3b. The main peaks in the spectra do not display any orientation dependence as we used different polarization angles. Plotting the data into a polar pattern reveals a semicircle shape for the C−C short axis mode and dots around the origin for the C−C long axis mode. These results not only indicate that the molecules do stand up in the vertical orientation, but also confirm that the preferred orientation of pentacene molecules observed in Figure 3a most likely is a direct consequence of the underlying presence of graphene on the copper substrate.

Formation of Pentacene Domains. Due to random nucleation, graphene grown on bare Cu foil by CVD method are intrinsically polycrystalline.[36−39] According to Figure 4, graphene act as a template layer for the alignment of pentacene molecules. To have a better understanding of the characteristics between the underlying polycrystalline graphene and pentacene, further investigation in different regions of the sample was performed. As shown in Figure 4a, after depositing pentacene film of 50 nm thick on graphene/Cu, three separate regions (highlighted by the white dashed line) were observed. Polar patterns of each region are shown in Figure 4b−d. These patterns arise from the C−C short axis mode of the Raman spectra of pentacene. We chose the C−C short axis mode to define the molecular orientation because of its (overall) higher anisotropy and intensity (the overall difference of short axis with polarization is more significant as can be shown from Figure 3). The corresponding orientation of C−C short axis mode is 162 ± 2°, 149 ± 2°, and 97 ± 0° for regions I, II, and III, respectively. This suggests that orientations of pentacene molecules do not have a random distribution, but rather, they form domains in accordance to the preferred orientation of a polycrystalline material.

Polarized Raman Spectra of Pentacene on Single Crystal Graphene. We believe that these domains are strongly correlated to the nature of the underlying graphene crystal structure. To demonstrate the idea, we used a single-crystal graphene as our template material. Exfoliated graphene provides a single domain graphene with large enough size as shown in Figure 4e for the purpose of our comparative measurement. Our hypothesis is that, on single domain graphene, the deposited pentacene orients similarly at various points on the single domain graphene. In the white dotted loop, a monolayer graphene (labeled in 1, 2, and 3) can be identified with a darker area (labeled in 4) which was incidentally folded from the other side. After depositing pentacene film under the same conditions, we have performed similar Raman measurements at regions 1−4 shown in Figure 4f−i. The resulting orientations of C−C short axis modes are 89 ± 2°, 90 ± 2°, 89 ± 2°, and 0 ± 2°, respectively. The configurations of these first three points share astonishingly similar characteristic features in their polar patterns. Not only the pentacene molecules show almost the same orientation, but also similar degree of anisotropy as well. For comparison, the orientation of pentacene on region 4 is perpendicular to those on the monolayer graphene. This result provides evidence that the nature of the graphene substrate (crystallinity or layer number) determines the molecular orientation of the pentacene molecules. Although, the overall preferred orientation of

DOI: 10.1021/acsphotonics.6b00074
ACS Photonics 2016, 3, 985−991

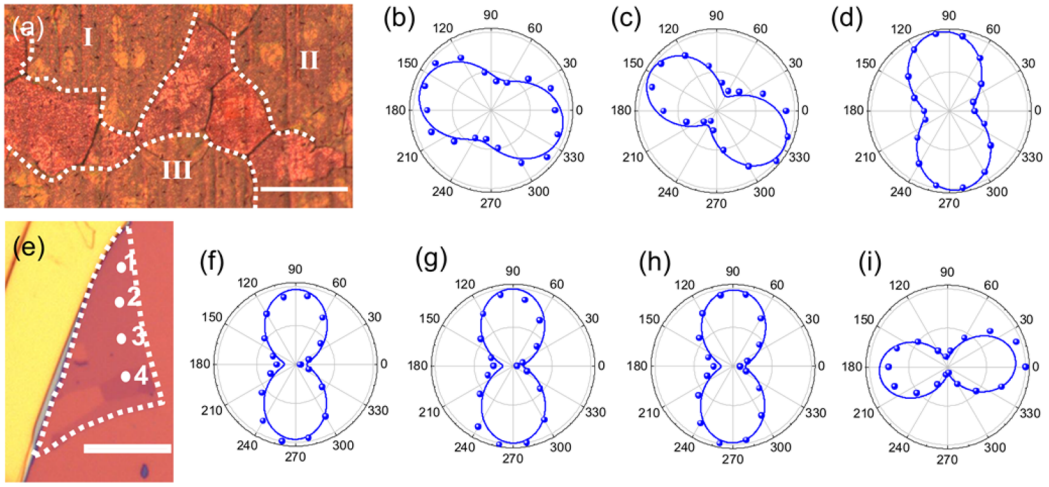

Figure 4. (a) Optical image of a pentacene film deposited on graphene/Cu substrate. The scale bar is 100 μm. There are three regions marked in I, II, and III bounded with white dashed line. The corresponding polar patterns of regions I, II, and III are shown in (b), (c), and (d). (e) Optical micrograph of an exfoliated graphene on SiO_2 shown in the white dotted loop. The scale bar is 20 μm. Raman polar plots obtained in regions numbered as 1, 2, 3, and 4 in (e) after depositing pentacene films are shown in (f), (g), (h), and (i), respectively. The solid blue curves are obtained from fitting the data of the C−C short axis mode.

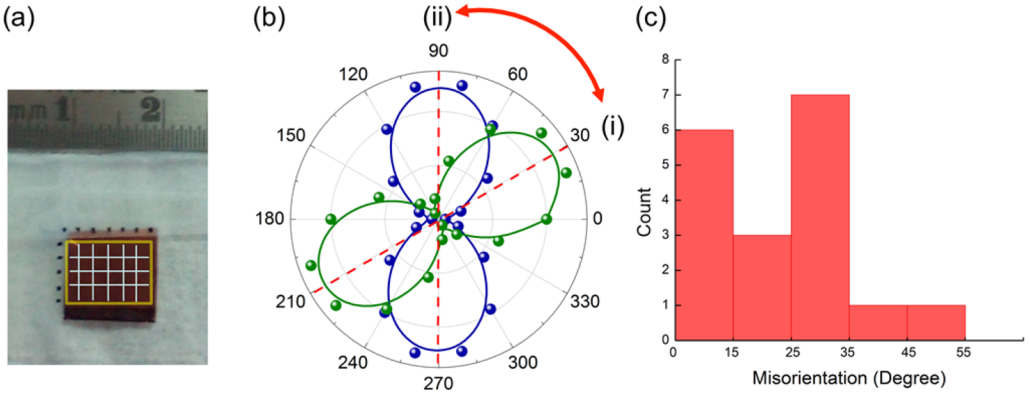

Figure 5. (a) Photographic image of a pentacene thin film deposited on graphene/Cu. The yellow rectangle encloses the area of Raman study, which is further divided by white lines into an overall of 24 mapping areas. Raman polar plots are obtained from each individual mapping area and compared between neighboring areas. (b) Definition of angles between two preferred orientations. The green curve is oriented about 30° (indicated with dashed red line in (i)) and the blue is 90° (shown in (ii)). The difference between angle (i) and (ii) is highlighted with a solid red curve. (c) Statistics of misorientaion between the neighboring areas in (a).

pentacene in $x-y$ plane is obvious for both poly- and single-crystal graphene substrate.

Visualization of Pentacene Domains on Graphene Surface. To have a closer inspection of the interaction between pentacene and graphene, we map out the orientation distribution of pentacene by obtaining spectra at different parts of the sample as shown in Figure 5a. The resulting polar pattern in each region gives a well-defined angle of preferred orientation. To investigate the angle-correlation of the ensemble, we measure the difference of angles between the neighboring areas, defined as the misorientation. For example, there is a preferred orientation of 30 degree marked as (i) and another of 90 deg labeled as (ii) in Figure 5b, the misorientation between these two areas is 60° and so on. The overall result is compiled in Figure 5c. It shows two peaks around 15° and 30°. Coincidentally, the generalized grain boundaries of graphene reported in literature have also been shown to exhibit misorientation of 16° and 29°, which is in good agreement with our observation.[40,41] An et al. discovered the predominant misorientation angles using transmission electron microscopic studies. Although, the origins of such misorientation angles were not yet clarified, they have pointed out that it may have conformed to the "coincident site lattices" (CSL) typically found in grain boundaries of polycrystalline materials. CSL values are used to indicate the stability of the grain boundary and related to the growth process of a crystal. Theoretically and experimentally, CSL values of graphite had been previously reported. Specifically, two CSL values at 19 and 13, have been confirmed to be present in the study of graphite.[42,43] The predominant misorientation angles of 15° and 30° observed in our samples can be correlated to the CSL. Interestingly, by simply probing the pentacene molecules present on top of our CVD graphene using polarized Raman spectroscopy, we have obtained crystallographic information on the latter material with similar information obtained from techniques such as TEM[44,45] and STM.[39,41] Therefore, it is clear that the polycrystalline graphene is a dominant factor in resulting discrete misorientation of pentacene domains.

Evolution of Pentacene Thin Films on Graphene/Cu. To understand the structural evolution of pentacene films

DOI: 10.1021/acsphotonics.6b00074
ACS Photonics 2016, 3, 985−991

grown on graphene/Cu, a comprehensive study of polarized Raman spectra has been conducted for various thicknesses of pentacene. The overall behavior of polarized Raman spectra of pentacene follows a sinusoidal function as mentioned above. As

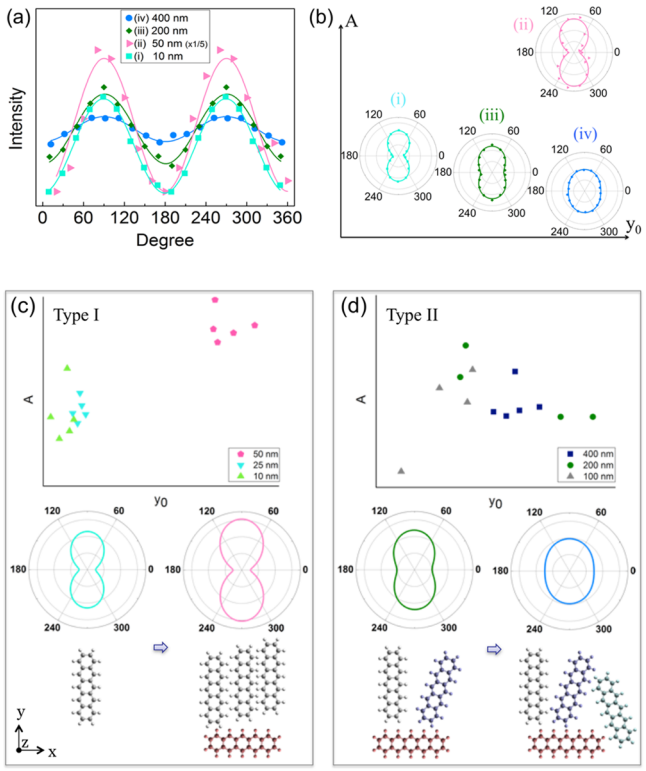

Figure 6. (a) Angle dependence of fitted curves with various combinations of A and y_0 values for pentacene films with different thicknesses. (b) Corresponding polar patterns of (i), (ii), (iii), and (iv) in (a). (c, d) Distribution of A and y_0 after fitting the experimental data of pentacene thin films at various thickness. The schematic below illustrates the main transition of polar pattern of each type and relative orientation of molecules viewed from the z-axis.

shown in Figure 6a, all Raman spectra can be fitted by the following empirical expression,

$$(A \sin \theta)^2 + y_0 \quad (2)$$

With larger A, the variation between maxima and minima becomes larger as shown in red and green curves, whereas y_0 serves as an upshift background signal arising from the random distribution of pentacene molecules. The corresponding polar patterns of the Raman spectra were plotted in Figure 6b. The significance of the parameters A and y_0 becomes more apparent in the polar patterns. Larger A appears to intensify the 8-shape structure, while larger y_0 opens the neck on the 8-shape and becomes eclipse-like. The distinct features of the shapes in Figure 6b happen to coincide with our measurements for different thicknesses. As observed from type I in Figure 6c and type II in Figure 6d, the distribution of each pattern has its own characteristic. In type I, $A-y_0$ relation increases with film thickness. In contrast, the $A-y_0$ relation in type II does not follow the same trend. Instead, they localize at similar level of A and y_0.

Based on these observations, we propose the structural evolution of the pentacene films in accordance with the polar patterns of Figure 6c,d. First, for a few layers of pentacene around 10−25 nm, the quantity of pentacene molecules is not high such that the orientation of most pentacene molecules is locked by the underlying substrate. Therefore, the Raman spectra show a strong anisotropic behavior and 8-shaped-like signals are observed. As the film grows to around 50 nm, the pentacene quantity is getting larger and the neck of the 8-shaped becomes obvious so as the signals of A and y_0. However, both A and y_0 cannot grow infinitely, instead they decrease and become saturated. Change of orientation (e.g., standing-up orientation) and the finite absorption depth may contribute to the saturation of the signals. The evolution of the thin film growth is illustrated in the lower panel of Figure 6c and d. In the first stage, a small amount of few molecules is well aligned, and then more molecules line up in the same fashion, while some molecules at different directions also stack together. The appearance of the other directions in $x-y$ plane strengthens y_0 and weakens A. Therefore, the role of A can serve as an indicator of the level of anisotropy and y_0 can be attributed to the degree of isotropy. The $A-y_0$ plot thus provides a clear view of the degree of anisotropy and also builds up a way to distinguish the evolution of different stacking modes at molecular level.

CONCLUSIONS

In summary, we have demonstrated that polarized Raman spectroscopy can be an effective way to determine the local orientation of pentacene film. This technique allows us to probe the relationship between the orientation of pentacene molecules and the substrate. It is found that, pentacene molecules are arranged in lying-down and standing-up configurations when deposited on CVD graphene on Cu and bare Cu foil, respectively. Moreover, the orientations of the lying-down pentacene molecules on CVD graphene form domains similar to the underlying polycrystalline graphene structure; in contrast, single-orientation pentacene film is observed on single crystal graphene. Also, the misorientation of graphene and pentacene domains shows obvious consistency. Our observation suggests that the orientation alignment of pentacene molecules is induced by the crystalline structure of graphene. It is found that the orientation of the domains of CVD graphene does not distribute randomly. Instead, the relative orientation of the nearby domain does exhibit preferred angles due to atomic interactions. Furthermore, we develop an $A-y_0$ plot, which can be use as an index in determining the degree of anisotropy for molecular packing. These results not only provide excellent route in terms of characterizing the domains of CVD graphene, which remains as a great challenge to overcome using existing techniques, but also a quantitative method that can be applicable to many other similar systems. In addition, the self-assembled behavior influenced by the underlying graphene could possibly enhance long-range aromatic molecular ordering, paving the way for novel device design.

METHODS

Materials and Fabrication. CVD was used for the growth of graphene. A polycrystalline Cu foil (purchased from Nilaco Inc.) was placed in a furnace and heated to 950 °C. H_2 was then passed into the quartz tube for 30 min prior to the introduction of CH_4. After the growth, CH_4 was switched off and the system

DOI: 10.1021/acsphotonics.6b00074
ACS Photonics 2016, 3, 985−991

was cooled in H_2 or Ar flow. The entire processes were operated at ~500 mTorr during the growth stage.

Single domain graphene was fabricated by mechanical exfoliation of graphene flakes onto the oxidized silicon wafer.

All pentacene (Aldrich, purity > 99%) films were deposited around 5×10^{-6} Torr from a glass crucible of a resistively heated cell at typical deposition rate of 0.2−0.4 Å/s, as determined by a quartz crystal balance.

Raman Measurements. Micro-Raman spectra were obtained using Horiba Jobin Yvon UV800 Raman spectrometer (resolution ~ 1 cm^{-1}) under the excitation of a laser with wavelength of 633 nm. The incident power was kept below 0.5 mW to avoid laser-induced heating. The laser spot is around 1 μm^2. The polarization of the incident beam is controlled by a half-wave plate taken at 20° rotation intervals. (Figures 5 and 6 were measured to 180°. To make the graph clearer, we use symmetrical characteristics for extension to 360°.) The polarization direction of the analyzer for the scattered light is fixed such that the angle-dependent effect on grating could be minimized.

■ ASSOCIATED CONTENT

Supporting Information

The Supporting Information is available free of charge on the ACS Publications website at DOI: 10.1021/acsphotonics.6b00074.

(S1) Structure of a pentacene molecule and the corresponding Raman tensor with polar patterns. (S2) Fitted polar pattern of Figure 3a (PDF).

■ AUTHOR INFORMATION

Corresponding Authors

*E-mail: chenlc@ntu.edu.tw.

*E-mail: yfchen@phys.ntu.edu.tw.

Notes

The authors declare no competing financial interest.

■ ACKNOWLEDGMENTS

We thank Dr. C. K. Chang and I. N. Chen for technical support and helpful discussions. This work was supported by the Ministry of Science and Technology in Taiwan using Grants 103-2745-M-002-006-ASP and 104-2745-M-002-004-ASP.

■ REFERENCES

(1) Tumbleston, J. R.; Collins, B. A.; Yang, L.; Stuart, A. C.; Gann, E.; Ma, W.; You, W.; Ade, H. The influence of molecular orientation on organic bulk heterojunction solar cells. *Nat. Photonics* **2014**, *8*, 385−391.

(2) Yokoyama, D. Molecular orientation in small-molecule organic light-emitting diodes. *J. Mater. Chem.* **2011**, *21*, 19187−19202.

(3) Lee, H. S.; Kim, D. H.; Cho, J. H.; Hwang, M.; Jang, Y.; Cho, K. Effect of the Phase States of Self-Assembled Monolayers on Pentacene Growth and Thin-Film Transistor Characteristics. *J. Am. Chem. Soc.* **2008**, *130*, 10556−10564.

(4) Jang, Y.; Cho, J. H.; Kim, D. H.; Park, Y. D.; Hwang, M.; Cho, K. Effects of the permanent dipoles of self-assembled monolayer-treated insulator surfaces on the field-effect mobility of a pentacene thin-film transistor. *Appl. Phys. Lett.* **2007**, *90*, 132104−1−132104−3.

(5) Veres, J.; Ogier, S. D.; Leeming, S. W.; Cupertino, D. C.; Khaffaf, S. M. Low-k Insulators as the Choice of Dielectrics in Organic Field-Effect Transistors. *Adv. Funct. Mater.* **2003**, *13*, 199−204.

(6) Rao, C. N. R.; Biswas, K. Characterization of Nanomaterials by Physical Methods. *Annu. Rev. Anal. Chem.* **2009**, *2*, 435−462.

(7) Malard, L. M.; Pimenta, M. A.; Dresselhaus, G.; Dresselhaus, M. S. Raman Spectroscopy in Graphene. *Phys. Rep.* **2009**, *473*, 51−87.

(8) Ferrari, A. C.; Basko, D. M. Raman Spetrocopsy as a Versatile Tool for Studying the Properties of Graphene. *Nat. Nanotechnol.* **2013**, *8*, 235−246.

(9) Ling, X.; Wu, J.; Xu, W.; Zhang, J. Probing the Effect of Molecular Orientation on the Intensity of Chemical Enhancement Using Graphene-Enhanced Raman Spectroscopy. *Small* **2012**, *8*, 1365−1372.

(10) Hwang, J.-S.; Lin, Y.-H.; Hwang, J.-Y.; Chang, R.; Chattopadhyay, S.; Chen, C.-J.; Chen, P.; Chiang, H.-P.; Tsai, T.-R.; Chen, L.-C.; Chen, K.-H. Imaging Layer Number and Stacking Order through Formulating Raman Fingerprints Obtained from Hexagonal Single Crystals of Few-layer Graphene. *Nanotechnology* **2013**, *24*, 015702−1−015702−10.

(11) Chang, C. K.; Kataria, S.; Kuo, C. C.; Ganguly, A.; Wang, B. Y.; Hwang, J. Y.; Huang, K. J.; Yang, W. H.; Wang, S. B.; Chuang, C. H.; Chen, M.; Huang, C. I.; Pong, W. F.; Song, K. J.; Chang, S. J.; Guo, J. H.; Tai, Y.; Tsujimoto, M.; Isoda, S.; Chen, C. W.; Chen, L. C.; Chen, K. H. Band Gap Engineering of Chemical Vapor Deposited Graphene by in-situ BN Doping. *ACS Nano* **2013**, *7*, 1333−1341.

(12) Pan, S.-H.; Medina, H.; Wang, S.-B.; Chou, L.-J.; Wang, Z. M.; Chen, K.-H.; Chen, L.-C.; Chueh, Y.-L. Direct Assessment of the Mechanical Modulus for Graphene Co-doped with Low Concentrations of Boron-Nitrogen by a Non-contact Approach. *Nanoscale* **2014**, *6*, 8635−8641.

(13) Mohiuddin, T. M. G.; Lombardo, A.; Nair, R. R.; Bonetti, A.; Savini, G.; Jalil, R.; Bonini, N.; Basko, D. M.; Galiotis, C.; Marzari, N.; Novoselov, K. S.; Geim, A. K.; Ferrari, A. C. Uniaxial Strain in Graphene by Raman Spectroscopy: *G* Peak Splitting, Grüneisen Parameters, and Sample Orientation. *Phys. Rev. B: Condens. Matter Mater. Phys.* **2009**, *79*, 205433−1−205433−8.

(14) Huang, M.; Yan, H.; Chen, C.; Song, D.; Heinz, T. F.; Hone, J. Phonon Softening and Crystallographic Orientation of Strained Graphene Studied by Raman Spectroscopy. *Proc. Natl. Acad. Sci. U. S. A.* **2009**, *106*, 7304−7308.

(15) Kim, D. W.; Kim, Y. H.; Jeong, H. S.; Jung, H.-T. Visualization of Large-area Graphene Domains and Boundaries by Optical Birefringency. *Nat. Nanotechnol.* **2011**, *7*, 29−34.

(16) Tanaka, M.; Young, R. J. Review Polarised Raman spectroscopy for the study of molecular orientation distributions in polymers. *J. Mater. Sci.* **2006**, *41*, 963−991.

(17) Ying Mao, H.; Wang, R.; Wang, Y.; Chao Niu, T.; Qiang Zhong, J.; Yang Huang, M.; Chen, Q. D.; Ping Loh, K.; Thye Shen Wee, A.; Chen, W. Chemical vapor deposition graphene as structural template to control interfacial molecular orientation of chloroaluminium phthalocyanine. *Appl. Phys. Lett.* **2011**, *99*, 093301−1−093301−3.

(18) Chen, W.; Qi, D. C.; Huang, H.; Gao, X.; Wee, A. T. S. Organic−Organic Heterojunction Interfaces: Effect of Molecular Orientation. *Adv. Funct. Mater.* **2011**, *21*, 410−424.

(19) Ruiz, R.; Choudhary, D.; Nickel, B.; Toccoli, T.; Chang, K. C.; Mayer, A. C.; Clancy, P.; Blakely, J. M.; Headrick, R. L.; Iannotta, S.; Malliaras, G. G. Pentacene Thin Film Growth. *Chem. Mater.* **2004**, *16*, 4497−4508.

(20) Hlawacek, G.; Teichert, C. Nucleation and Growth of Thin Films of Rod-like Conjugated Molecules. *J. Phys.: Condens. Matter* **2013**, *25*, 143202.

(21) Cheng, H. L.; Mai, Y. S.; Chou, W. Y.; Chang, L. R.; Liang, X. W. Thickness-Dependent Structural Evolutions and Growth Models in Relation to Carrier Transport Properties in Polycrystalline Pentacene Thin Films. *Adv. Funct. Mater.* **2007**, *17*, 3639−3649.

(22) Cheng, H.-L.; Liang, X.-W.; Chou, W.-Y.; Mai, Y.-S.; Yang, C.-Y.; Chang, L.-R.; Tang, F.-C. Raman Spectroscopy Applied to Reveal Polycrystalline Grain Structures and Carrier Transport Properties of Organic Semiconductor Films: Application to Pentacene-based Organic Transistors. *Org. Electron.* **2009**, *10*, 289−298.

(23) James, D. T.; Kjellander, B. K. C.; Smaal, W. T. T.; Gelinck, G. H.; Combe, C.; McCulloch, I.; Wilson, R.; Burroughes, J. H.; Bradley, D. D. C.; Kim, J. S. Thin-Film Morphology of Inkjet-Printed Single-

DOI: 10.1021/acsphotonics.6b00074
ACS Photonics 2016, 3, 985−991

Droplet Organic Transistors Using Polarized Raman Spectroscopy: Effect of Blending TIPS-Pentacene with Insulating Polymer. *ACS Nano* **2011**, *5*, 9824−9835.
(24) Hunter, C. A.; Sanders, J. K. M. The Nature of $\pi-\pi$ Interactions. *J. Am. Chem. Soc.* **1990**, *112*, 5525−5534.
(25) Chen, W.; Huang, H.; Thye, A.; Wee, S. Molecular orientation transition of organic thin films on graphite: the effect of intermolecular electrostatic and interfacial dispersion forces. *Chem. Commun.* **2008**, *36*, 4276−4278.
(26) Zheng, Y.; Qi, D.; Chandrasekhar, N.; Gao, X.; Troadec, C.; Wee, A. T. S. Effect of Molecule-Substrate Interaction on Thin-Film Structures and Molecular Orientation of Pentacene on Silver and Gold. *Langmuir* **2007**, *23*, 8336−8342.
(27) Lukas, S.; Söhnchen, S.; Witte, G.; Wöll, C. Epitaxial Growth of Pentacene Films on Metal Substrates. *ChemPhysChem* **2004**, *5*, 266−270.
(28) Götzen, J.; Käfer, D.; Wöll, C.; Witte, G. Growth and Structure of Pentacene Films on Graphite: Weak Adhesion As a Key for Epitaxial Film Growth. *Phys. Rev. B: Condens. Matter Mater. Phys.* **2010**, *81*, 085440−1−085440−12.
(29) France, C. B.; Schroeder, P. G.; Parkinson, B. A. Direct Observation of a Widely Spaced Periodic Row Structure at the Pentacene/Au(111) Interface Using ScanningTunneling Microscopy. *Nano Lett.* **2002**, *2*, 693−696.
(30) Djuric, T.; Ules, T.; Flesch, H. G.; Plank, H.; Shen, Q.; Teichert, C.; Resel, R.; Ramsey, M. G. Epitaxially Grown Films of Standing and Lying Pentacene Molecules on Cu(110) Surfaces. *Cryst. Growth Des.* **2011**, *11*, 1015−1020.
(31) Berke, K.; Tongay, S.; McCarthy, M. A.; Rinzler, A. G.; Appleton, B. R.; Hebard, A. F. Epitaxially Grown Films of Standing and Lying Pentacene Molecules on Cu(110) Surfaces. *J. Phys.: Condens. Matter* **2012**, *24*, 255802.
(32) Huang, S.; Ling, X.; Liang, L.; Song, Y.; Fang, W.; Zhang, J.; Kong, J.; Meunier, V.; Dresselhaus, M. Molecular Selectivity of Graphene-Enhanced Raman Scattering. *Nano Lett.* **2015**, *15*, 2892−2901.
(33) Turrell, G. In *Practical Raman Spectroscopy SE - 2*; Gardiner, D., Graves, P., Eds.; Springer−Verlag: Berlin, 1989; pp 13−54.
(34) Mino, T.; Saito, Y.; Yoshida, H.; Kawata, S.; Verma, P. Molecular Orientation Analysis of Organic Thin Films by Z-polarization Raman Microscope. *J. Raman Spectrosc.* **2012**, *43*, 2029−2034.
(35) Presser, V.; Schuster, B. E.; Casu, M. B.; Heinemeyer, U.; Schreiber, F.; Nickel, K. G.; Chassé, T. Raman Polarization Studies of Highly Oriented Organic Thin Films. *J. Raman Spectrosc.* **2009**, *40*, 2015−2022.
(36) Yu, Q.; Jauregui, L. A.; Wu, W.; Colby, R.; Tian, J.; Su, Z.; Cao, H.; Liu, Z.; Pandey, D.; Wei, D.; Chung, T. F.; Peng, P.; Guisinger, N. P.; Stach, E. A.; Bao, J.; Pei, S.-S.; Chen, Y. P. Control and Characterization of Individual Grains and Grain Boundaries in Graphene Grown by Chemical Vapour Deposition. *Nat. Mater.* **2011**, *10*, 443−449.
(37) Biró, L. P.; Lambin, P. Grain Boundaries in Graphene Grown by Chemical Vapor Deposition. *New J. Phys.* **2013**, *15*, 035024.
(38) Huang, P. Y.; Ruiz-Vargas, C. S.; van der Zande, A. M.; Whitney, W. S.; Levendorf, M. P.; Kevek, J. W.; Garg, S.; Alden, J. S.; Hustedt, C. J.; Zhu, Y.; Park, J.; McEuen, P. L.; Muller, D. A. Grains and Grain Boundaries in Single-layer Graphene Atomic Patchwork Quilts. *Nature* **2011**, *469*, 389−392.
(39) Kim, K.; Lee, Z.; Regan, W.; Kisielowski, C.; Crommie, M. F.; Zettl, A. Grain Boundary Mapping in Polycrystalline Graphene. *ACS Nano* **2011**, *5*, 2142−2146.
(40) Yazyev, O. V.; Chen, Y. P. Grain Boundary Mapping in Polycrystalline Graphene. *Nat. Nanotechnol.* **2014**, *9*, 755−767.
(41) An, J.; Voelkl, E.; Suk, J. W.; Li, X.; Magnuson, C. W.; Fu, L.; Tiemeijer, P.; Bischoff, M.; Freitag, B.; Popova, E.; Ruoff, R. S. Domain (Grain) Boundaries and Evidence of "Twinlike" Structures in Chemically Vapor Deposited Grown Graphene. *ACS Nano* **2011**, *5*, 2433−2439.
(42) Minkoff, I.; Myron, S. Rotation Boundaries and Crystal Growth in the Hexagonal System. *Philos. Mag.* **1969**, *19*, 379−387.
(43) Bleris, G. L.; Nouet, G.; Hagège, S.; Delavignette, P. Characterization of Grain-Boundaries in the Hexagonal System Based on Tables of Coincidence Site Lattices (CSLs). *Acta Crystallogr., Sect. A: Cryst. Phys., Diffr., Theor. Gen. Crystallogr.* **1982**, *38*, 550−557.
(44) Lahiri, J.; Lin, Y.; Bozkurt, P.; Oleynik, I. I.; Batzill, M. An extended defect in graphene as a metallic wire. *Nat. Nanotechnol.* **2010**, *5*, 326−329.
(45) Cockayne, E.; Rutter, G. M.; Guisinger, N. P.; Crain, J. N.; First, P. N.; Stroscio, J. A. Grain boundary loops in graphene. *Phys. Rev. B: Condens. Matter Mater. Phys.* **2011**, *83*, 195425−1−195425−7.

DOI: 10.1021/acsphotonics.6b00074
ACS Photonics 2016, 3, 985−991